35th Annual International Conference of the IEEE EMBS
Osaka, Japan, 3 - 7 July, 2013

Area Stenosis Associated with Non-Invasive Fractional Flow Reserve Obtained from Coronary CT Images *

Jun-Mei Zhang, Tong Luo, Yunlong Huo, Min Wan, Terrance Chua, Ru San Tan, Ghassan S. Kassab, Swee Yaw Tan, and Liang Zhong

Abstract—**Fractional flow reserve (FFR) determined by invasive angiography is the gold standard to assess the severity of coronary artery disease (CAD). FFR_{CT} can be obtained non-invasively by combining computed tomography (CT) images and Computational Fluid Dynamics (CFD) method. In this study, FFR_{CT} was computed for 6 models of patient-specific left coronary artery trees reconstructed from CT images. A total of 12 stenoses were observed. FFR values obtained for 7 of the 12 stenoses during invasive angiography were used as the gold standard for comparison. On a per-stenosis basis, the sensitivity, specificity, positive predictive value and negative predictive value were 50%, 100%, 100% and 83.3% respectively for FFR_{CT}. A weak correlation was found between percent lumen diameter stenosis and FFR_{CT} ($r=0.431$; $p>0.05$). However, the correlation between percent lumen area stenosis and FFR_{CT} was significant ($r=0.853$; $p<0.05$). Therefore, non-invasive FFR_{CT} appears to be a promising index to assess the severity of CAD and lumen area has distinct advantages over diameter measurement in terms of anatomy assessment.**

*Research supported by National Medical Research Council, (NMRC/EDG/1037/2011) and SingHealth (SHF/FG503P/2012).

Jun-Mei Zhang is with the Cardiac Mechanics Engineering and Physiology Unit, National Heart Center, Singapore, Mistri Wing 17, 3rd Hospital Avenue, 168752, Singapore (e-mail: zhang.junmei@nhcs.com.sg; zhangjunmei@gmail.com).

Tong Luo is with the Departments of Biomedical Engineering, Surgery, and Cellular and Integrative Physiology, Indiana University Purdue University Indianapolis, Indianapolis, IN 46202, USA (e-mail: tongluo@iupui.edu).

Yunlong Huo is with the Department of Mechanics and Engineering Science, College of Engineering, Peking University, Beijing, 100871, China (e-mail: yhuo@pku.edu.cn)

Min Wan is with the Cardiac Mechanics Engineering and Physiology Unit, National Heart Center, Singapore, Mistri Wing 17, 3rd Hospital Avenue, 168752, Singapore (e-mail: wan.min@nhcs.com.sg).

Terrance Chua is with the Cardiology Department, National Heart Center, Singapore, Mistri Wing 17, 3rd Hospital Avenue, 168752, Singapore (e-mail: terrance.chua.s.j@nhcs.com.sg).

Ru San Tan is with the Cardiology Department, National Heart Center, Singapore, Mistri Wing 17, 3rd Hospital Avenue, 168752, Singapore (e-mail: tan.ru.san@nhcs.com.sg).

Ghassan S. Kassab is with the Departments of Biomedical Engineering, Surgery, and Cellular and Integrative Physiology, Indiana University Purdue University Indianapolis, Indianapolis, IN 46202, USA (e-mail: gkassab@3dtholdings.com).

Swee Yaw Tan is with the Cardiology Department, National Heart Center, Singapore, Mistri Wing 17, 3rd Hospital Avenue, 168752, Singapore (e-mail: tan.swee.yaw@nhcs.com.sg).

Liang Zhong is with the Cardiac Mechanics Engineering and Physiology Unit, National Heart Center, Singapore, Mistri Wing 17, 3rd Hospital Avenue, 168752, Singapore (corresponding author, phone: 65- 64367682; fax: 65-62230972; e-mail: zhong.liang@nhcs.com.sg).

I. INTRODUCTION

Cardiovascular disease is the leading cause of death in the United States, and accounts for 17% of overall deaths [1]. In Singapore, 1 out of 3 deaths are due to heart disease or stroke [2]. Coronary vascular dysfunction has been linked to the development of cardiovascular-related events, such as death, myocardial infarction (MI), stroke and unstable angina [3]. A series of imaging techniques have been used to assess the severity of coronary artery disease (CAD), including myocardial contrast echocardiography, contrast computed tomography (CT) and so on [4]. To quantify the anatomical significance of stenosis, diameter stenosis (DS) percentage is usually reported by these imaging techniques. Other imaging techniques, including positron emission tomography (PET), cardiac magnetic resonance and so on, have been used to quantify the absolute flow and myocardial or coronary flow reserve (CFR). Recent years, fractional flow reserve (FFR) has been used as the gold standard to guide percutaneous coronary intervention (PCI), as it leads to significantly fewer follow-up coronary events than PCI based on angiographic percent stenosis [5].

In general, 3 kinds of indicators are commonly used in the clinic to quantify the significance of CAD, namely DS, CFR and FFR. The first one reveals the anatomical significance of the stenosis, while the last two assess coronary physiology from the viewpoints of flow and pressure separately. However, these indicators are reported to be discordant for many cases. Quantitative DS percentage is reported to be poorly related to either CFR [6] or FFR [7]. As the coronary lumen deviates from circular geometry in disease, the lumen area stenosis (AS) is thought to have distinct advantages over DS and may be better correlated with physiological parameter.

Among the physiological parameters, FFR has been used as the gold standard to assess the significance of CAD. However, it is invasive and the results are negative in the majority of patients with obstructive CAD [4]. With the advancement of CFD technologies, numerical simulation has been used to study CAD. Kim and colleagues [8, 9] simulated patient-specific coronary arteries with sophisticated lumped parameter models. Based on their CFD technologies, non-invasive FFR_{CT} was derived from CT imagines and it was demonstrated to have high diagnostic performance [10]. As the invasive measurement of FFR is based on the mean pressure and the determination of the numerous parameters introduced in the lumped parameter models [10] is confusing, in this study the FFR_{CT} was obtained by CFD simulation on steady state with simplified resistance boundary conditions at

the outlets to reduce the computational cost. To test its accuracy, non-invasive FFR_{CT} was obtained for 6 models of patient-specific left coronary artery trees reconstructed from CT images. The FFR_{CT} values were compared with the FFR values obtained through invasive angiography. In addition, the relationship of FFR_{CT} with coronary DS and AS was investigated separately.

II. METHODS

A. CT Scans and Images Processing

As a prospective pilot study, 6 patients (aged between 45 to 64 years old) with atypical angina pain were examined on a 64-slice Toshiba Aquilion Multidetector CT scanner. After an initial non-contrast enhanced scan for calcium scoring, the patients were injected with contrast agent, which were controlled with bolus tracking.

The scan parameters were slice acquisition: 64×0.5 mm; gantry rotation time: 350 ms; tube potential: 120 kV. Depending on the cardiac dimensions and pitch, scanning time was 5.7–8.4 s, in a single breath hold in the craniocaudal direction. A representative CT image is shown in Fig. 1. All the CT images were recorded with a slice thickness of 0.5 mm and an increment of 0.25 mm. The pixel spacing was 0.439×0.439 mm and the field of view (FOV) was 225mm^2.

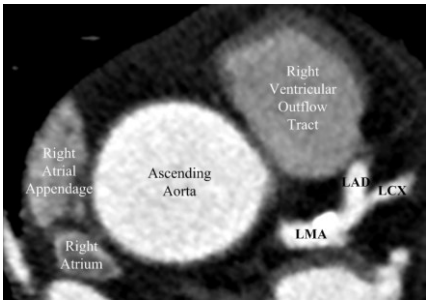

Figure 1. Single, transverse slice from the original CT data set. The major segmentations of the left coronary tree can be seen. LMA, left main coronary artery; LAD, left anterior descending artery; LCX, left circumflex artery.

Following CT scans, the artery structure was segmented from the background image to reconstruct 3D coronary tree. The Hessian matrix based filter was applied to each single transverse CT image for obtaining the high order geometric characteristics, i.e. principal curvature of the image intensity [11]. Based on the eigenvector analysis of the obtained Hessian matrix, the decision could be made if the voxel being analyzed belonged to the vessel structure or not.

Enhancement was done upon the voxel more likely from the vessel structure. The graph-cuts based image segmentation technique [12] was then applied to the enhanced 3D image. Marching cube algorithm was used to establish the triangulated surface mesh from segmented voxel data. A reconstructed left coronary artery tree model was shown in Fig. 2 with an enlarged view of 4 stenoses on the left anterior descending artery (LAD), namely A, B, C and D separately.

The detailed topology of these 4 stenoses at different views was shown in Fig. 3. As it can be seen, the coronary lumens were far from circular at the stenosis regions. Therefore lumen area assessment was believed to have distinct advantages over diameter measurements, as it has less dependency on viewing angle and reference sites [13]. By refining the image processing techniques used in this study, we could produce the lumen area stenosis ratio besides the diameter stenosis ratio for every stenosis and thus enable the study of the effect of area stenosis on hemodynamics. The reconstructed coronary artery tree was used for further CFD simulation.

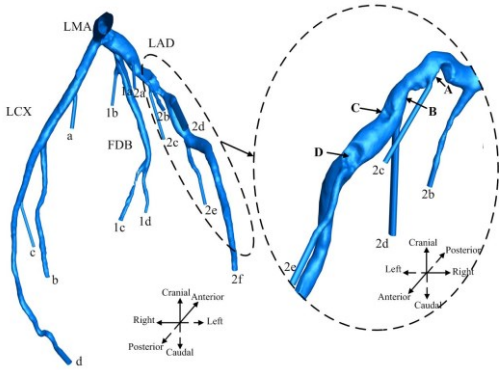

Figure 2. Reconstructed left coronary artery tree model with primary branches (≥ 1.0mm in diameter). Enlarged view of 4 stenoses on the LAD is shown in the inset with rotated coordinate system. a-d are the branches for LCX, 1a -1d are branches for FDB (first diagonal branch of the LAD) and the 2a-2f are the branches for the rest of the LAD. A-D are stenoses observed on LAD.

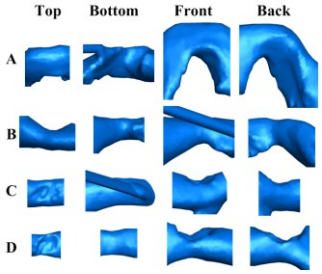

Figure 3. Stenosis A, B, C and D at different views

B. CFD Simulation on the Hemodynamics in Patient-specific Models

Commercial software ANSYS workbench was used in this study to discretize the flow domain with tetrahedral shaped elements. Finer meshes were located near the branch junctions, stenosis and the wall for fine resolution. A total of around 1.1 million volume cells were required for every patient-specific model to accurately discretize the computational domain after the grid-independency test.

As the comparisons of pulsatile and steady-state flows showed a negligible difference for coronary artery [14], the flow in the 6 patient-specific left coronary artery trees was assumed to be steady in this study. The continuity and Navier-Stokes equations (as shown in (1) and (2)) were solved to simulate the blood flow in the models.

$$\frac{\partial \rho u_i}{\partial x_i} = 0 \tag{1}$$

$$\frac{\partial}{\partial x_i}(\rho u_i u_j) = -\frac{\partial p}{\partial x_i} + \mu \frac{\partial^2 u_i}{\partial x_j^2} \tag{2}$$

Here x_i was the location in Cartesian coordinate, u_i was Cartesian component of velocity, p was the static pressure. ρ and μ were density and laminar viscosity. They were assigned as 1060 kg/m^3 and 4.5×10^{-3} Pa○s respectively to mimic the blood flow in large epicardial arteries.

The boundary conditions were set to be as close as possible to the real physiological condition. For example, the resting total coronary blood flow was calculated from the measured myocardial mass [15]. The distribution of the resting blood flow among normal coronary arteries (without stenosis) was assumed to obey the scale law [16]. Based on the patient-specific mean pressure and resting coronary blood flow, the resistance of each coronary branch was obtained. As the resistances of the downstream vasculature are decided by its own anatomy rather than the upstream structures, the same resistance values are applicable to the model with stenosis. At hyperemic condition, the resistance of the coronary arteries was reduced and the inflow rate of the left coronary artery tree was increased accordingly [17]. Therefore at the inlet, the patient-specific hyperemic flow rate was supplied, while patient-specific resistance boundary conditions were supplied at the outlets by compiling user defined functions (UDF) to the solver. Here the resistance values R_i was defined as $(P_i\text{-}P_0)/Q_i$, where P_i represented the pressure value at the outlet. P_0 represented the pressure at the right atrium (central venous pressure) and was estimated as 4.6 mmHg in this study [18]. To ensure smooth convergence, the pressure gradient calculated at the outlets was attenuated five times to couple iterative under-relaxation-based resistance boundary conditions with those outlets.

All walls were assumed to be non-slip. All computations were executed in a Dell T7500 workstation.

III. Results

To explore the effect of stenosis on flow pattern, Fig. 4(a) shows representative 3D streamlines for a patient-specific model. Along the LCX branch, the blood flows downstream smoothly due to the absence of stenosis. After flow passing the first diagonal branch (FDB), the derivations of streamlines are observed along LAD due to the disturbed flow resulted from the stenoses. At each stenosis region, the lumen cross-sectional area is reduced and hence the velocity magnitude is increased.

Accordingly, blood pressure drops much more after passing stenoses along the LAD than the LCX (as shown in Fig. 4(b)) due to larger decrease of momentum, which can be explained by Poiseuile equation. It is worth noting that the FFR_{CT} in Fig. 4(b) represents the pressure ratio of distal pressure over the aortic pressure[10], which is derived from the CFD simulation results.

This kind of pressure distribution is in line with the clinical observations that the diseased artery has lower FFR values than that of the normal vessel.

There are a total of 12 stenoses for the 6 patient-specific left coronary artery tree models investigated in this study. FFR value was obtained only for 7 of the 12 stenoses by invasive angiograph. Therefore Fig. 5 (a) shows the relationship between FFR and FFR_{CT} values for 7 stenoses. 0.8 is used as the threshold for both FFR and FFR_{CT}: stenosis having a value larger than 0.8 is predicted to be negative and vice versa. Only two of the 7 stenoses were predicted to be positive according to their FFR values, while the rest are negative. According to FFR_{CT} values, only one of 7 stenoses was predicted to be positive. Although the predicted FFR_{CT} values of each of these 7 stenoses does not match the corresponding FFR values exactly, five of seven are classified in the same category. On a per-stenosis basis, the sensitivity, specificity, positive predictive value and negative predictive value were 50%, 100%, 100% and 83.3% respectively for FFR_{CT}. Therefore the FFR_{CT} obtained from the combination of CT and CFD methods are almost consistent with the gold standard of FFR. As the latter must be obtained by invasive angiography, FFR_{CT} is a promising clinical diagnostic index to assess the significance of CAD, which can reduce the need for invasive angiography and medical cost.

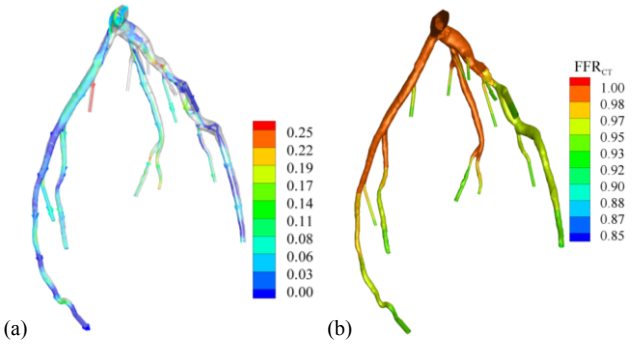

Figure 4. (a) 3-D streamlines with color bar to show the magnitude of velocity (m/s) and (b) pressure distribuition over a patient-specific left coronary artery tree model

The relationships between FFR_{CT} with diameter and area stenosis are shown in Fig. 5(b) and (c) respectively. As can be seen, FFR_{CT} values decrease with increase of either diameter or area stenosis percentage. This can be understood as the pressure drop becomes much more significant after passing over a severe stenosis than a lesser one.

A liner curve can be fitted for the data in both Figs. 5(b) and (c) and the correlation between FFR_{CT} and area stenosis ratio ($r=0.853$; $p<0.05$) is significant, unlike that for diameter stenosis ($r=0.431$; $p>0.05$) (Table 1). Lumen area stenosis has better correlation with indices of hemodynamics significance, as convective and diffusive energy losses due to the constriction and sudden expansion of the lumen area distal to stenosis result in essential pressure drop over stenosis regions [14]. This further affirms that it may be necessary and preferable to establish routine lumen area stenosis assessment in clinical practice.

TABLE I. The Relationship between FFR_{CT} and Area and Diameter Stenosis

	FFR_{CT} ~ Diameter Stenosis Ratio	**FFR_{CT} ~ Area Stenosis Ratio**
Intercept/Standard Error	1.0924/0.0999	1.0867/0.0343
Slope/Standard Error	-0.00334/0.00178	$-0.00306/5.565\times10^{-4}$
r	0.431	0.853
p	>0.05	<0.05

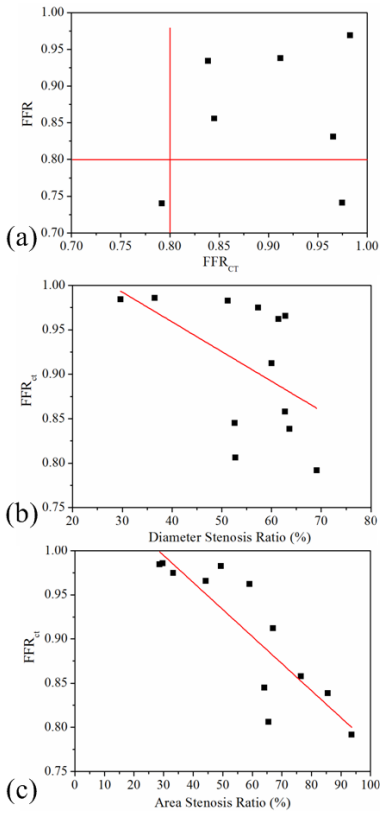

Figure 5. The reslationship (a) between FFR and FFR_{CT} for 7 stenoses and the relationship of FFR_{CT} with (b) diameter and (c) area stenosis ratio for a total of 12 stenosis

IV. Conclusion

In this study, non-invasive FFR_{CT} for 6 patient-specific left coronary artery trees were obtained by combining CT images and Computational Fluid Dynamics (CFD) methods. On a per-stenosis basis, the FFR_{CT} produced only 1 false negative value out of the total negative values of 6, using the FFR values obtained by invasive angiography as gold standard. Therefore FFR_{CT} is believed to be a promising index to assess the severity of CAD, as it bridges the anatomy to hemodynamic significance. However, investigations on larger population are necessary before making a final conclusion. In contrast to diameter stenosis ($r=0.431$; $p>0.05$), lumen area stenosis has much more significant correlation with FFR_{CT} ($r=0.853$; $p<0.05$), which affirms the importance of establishing routine lumen area stenosis assessment in clinical practice. This is applicable by advancing the image processing techniques used in this study.

Acknowledgment

This research is supported by the SingHealth Foundation, Singapore under its Translational Research Grant and administered by the SingHealth (SHF/FG503P/2012). The support of the National Medical Research Council (NMRC/EDG/1037/2011) is gratefully acknowledged.

References

[1] P. A. Heidenreich, J. G. Trogdon, O. A. Khavjou, J. Butler, K. Dracup, M. D. Ezekowitz, E. A. Finkelstein, Y. L. Hong, S. C. Johnston, A. Khera, D. M. Lloyd-Jones, S. A. Nelson, G. Nichol, D. Orenstein, P. W. F. Wilson and Y. J. Woo, "Forecasting the future of cardiovascular disease in the United States a policy statement from the American heart association," *Circulation*, vol. 123, no. 8, pp. 933-944, January, 2011.

[2] Registrar-general Registry of Births & Deaths Immigration & Checkpoints Authority Singapore, "Registry of births and deaths 2011," *Singapore Demographic Bulletin*, January 2012.

[3] T. Heitzer, T. Schlinzig, K. Krohn, T. Meinertz and T. Műnzel, "Endothelial dysfunction, oxidative stress and risk of cardiovascular events in patients with coronary artery disease," *Circulation*, vol. 104, pp. 2643-2678, Nov. 2001.

[4] N. P. Johnson, R. L. Kirkeeide and K. L. Gould, "Is discordance of coronary flow reserve and fractional flow reserve due to methodology or clinically relevant coronary pathophysiology?" *JACC Cardiovascular Imaging*, vol. 5(2), pp. 193-202, Feb. 2012.

[5] P. A. L. Tonino, B. De Bruyne, N. H. J. Pijls, U. Siebert, F. Ikeno, M. Van't Veer, V . Klauss, G. Manoharan, T. Engstrom, K. G. Oldroyd, P. N. V. Lee, P. A. MacCarthy and W. F. Fearon, "Fractional flow reserve versus angiography for guiding percutaneous coronary intervention," *N Engl J Med*, vol. 360, pp. 213-224, Jan. 2009.

[6] C. W. White, C. B. Wright, D. B. Doty, L. F. Hiratza, C. L. Eastham, D. G. Harrison and M. L. Marcus, "Does visual interpretation of the coronary arteriogram predict the physiologic importance of a coronary stenosis?" *N Engl J Med*, vol. 310, pp. 819-824, 1984.

[7] K. L. Gould and N. P. Johnson, "Percent stenosis in CAD – a flaw in current practice," *Nature Reviews Cardiology*, vol. 7, no. 9, pp. 482-484, Sep. 2010.

[8] H. J. Kim, I. E. Vignon-Clementel, C. A. Figueroa, J. F. LaDisa, K. E. Jansen, J. A. Feinstein and C. A. Taylor, "On coupling a lumped parameter heart model and a three-dimensional finite element aorta model," *Ann Biomed Eng.*, vol. 37(11), pp. 2153-69, 2009.

[9] H. J. Kim, I. E. Vignon-Clementel, J. S. Coogan, C. A. Figueroa, K. E. Jansen and C. A. Taylor, "Patient-specific modeling of blood flow and pressure in human coronary arteries," *Ann Biomed Eng.*, vol. 38(10), pp. 3195-209, 2010.

[10] B-K. Koo, A. Erglis, J-H. Doh, D. V. Daniels, S. Jegere, H.-S. Kim, A. Dunning and T. DeFrance, A. Lansky, J. Leipsic and J. K. Min, "Diagnosis of ischemia-causing coronary stenoses by noninvasive fractional flow reserve computed from coronary computed tomographic angiograms. Results from the prospective multicenter DISCOVER-FLOW (Diagnosis of Ischemia-Causing Stenoses Obtained Via Noninvasive Fractional Flow Reserve)," *J Am Coll Cardiol.*, vol. 58(19), pp. 1989-1997, 2011.

[11] T. Koller, G. Gerig, G. Székely and D. Dettwiler, "Multiscale detection of curvilinear structures in 2D and 3D image data," in *Proc. IEEE Int. Conf. Comput. Vision*, Los Alamitos, Calif, 1995, pp. 864–869.

[12] Y. Boykov, O. Veksler, and R. Zabih, "Fast approximate energy minimization via graph cuts," *IEEE Transactions on Pattern Analysis and Machine Intelligence*, vol. 23, no. 11, pp. 1222–1239, Nov. 2001.

[13] A. Arbab-Zadeh, "Quantification of coronary arterial stenoses by multidetector CT angiography in comparison with conventional angiography," *J. Am. Coll Cardiol.*, vol. 42, no. 2, pp. 191-202, Feb. 2011.

[14] Y. Huo, M. Svendsen, J. S. Choy, Z. D. Zhang and G. S. Kassab, "A validated predictive model of coronary fractional flow reserve," *J. R. Soc. Interface*, vol. 9, no. 71, pp. 1325-38, June 2012.

[15] M. Hamada, T. Kuwahara, Y. Shigematsu, K. Kodama, Y. Hara, H. Hashida, S. Ikeda, T. Ohtsuka, S. Nakata and K. Hiwada, "Relation between coronary blood flow and left ventricular mass in hypertension: noninvasive quantification of coronary blood flow by Thallium-201 myocardial scintigraphy," *Hypertens Res.*, vol. 21, no. 4, pp. 227-233, Dec. 1998.

[16] Y. F. Zhou, G. S. Kassab and S. Molloi, "On the design of the coronary arterial tree: a generalization of Murray's law," *Phys. Med. Biol.*, vol. 44, no. 12, pp. 2929–2945, Dec. 1999.

[17] R. F. Wilson, K. Wyche, B. V. Christensen, S. Zimmer and D. D. Laxson, "Effects of adenosine on human coronary arterial circulation," *Circulation*, vol. 82, no. 5, pp. 1595-1606, Nov. 1990.

[18] W. F. *Ganong Review of medical physiology*. New York : McGraw-Hill Medical, 2010, pp. 475.